CONTROL OF PREDETONATION EXPLOSION PROCESSES IN PROPELLANTS

A. A. Sulimov and B. S. Ermolaev

Deflagration-to-detonation transition in porous propellants includes two predetonation intermediate stages: convective burning (CB) and low-velocity detonation. This paper summarizes the results of experimental and theoretical studies of CB stabilization and control. Quasisteady modes of CB in propellants with low porosity (2–10%) are analyzed. The spatial structure of a CB-wave, stabilization mechanisms, characteristics of quasisteady CB, and the factors effecting the rate of chemical transformation in the burning zone (within the range of CB velocity 1–200 m/s) are discussed. The experimental data illustrating the specific features of the processes are discussed and the effects of the initial properties of charges are considered. The experimental data are compared with the results of calculation. Also discussed are applications of CB in low-porosity propellants for increasing the efficiency of propulsion and barrel systems.

INTRODUCTION

Deflagration-to-detonation transition (DDT) is a complex multistage process which, in general, comprises four stages: initial layer-by-layer burning governed by heat conduction, two intermediate processes — CB and low-velocity detonation (LVD), and the final stage of explosion development, that is normal detonation. The stages differ by the mechanisms of reaction initiation and energy transfer and by the ranges of propagation velocities and pressures.

The term "convective burning" normally applies to flame propagation in gas permeable energetic materials (EM). The mechanism of CB is associated with the filtration of the gaseous combustion products through pores and also with convective ignition of the porous EM. Convective burning, which provides penetration of combustion inward the EM and creates the conditions for the detonation-like mode of spreading the chemical reaction, is one of the most important stages in DDT. The traditional treatment of CB, as a nonsteady accelerating process, stems from the investigations of both explosion development in fine grained

explosives in a closed vessel and flame permeation into cracks in solid rocket propellants [1]. Therefore, determining the conditions under which CB can be stabilized, as well as studying the properties of stabilized CB, is attractive not only as an interesting theoretical problem, but will enable one to solve a number of practical explosion safety and applied problems. Before the works of the present authors, there were quite meagre data on the stabilized CB, which were obtained in experiments with short charges of high explosives of loose-packed density (or close to it) [2–4].

In our investigations [5–8], EM of low porosity (5 to 12%) and specially designed combustion chambers, equipped with an afterburning section and a nozzle, were used. These combustion chambers permitted simultaneous monitoring of flame propagation (by photography) and pressure variations at several sites distributed along the charge length and in the afterburning section (by means of piezoquartz pressure gauges). These studies revealed a burning mode with the average velocity of the CB-wave and the maximum pressure remaining nearly constant along fairly long charges, at the pressure in the afterburning section being constant. This process was referred to as the quasisteady CB. The performed studies furnished the data that shed light on the mechanism and spatial structure of CB-waves and on the mechanism and conditions of CB stabilization that preclude spontaneous flame acceleration and pressure build-up. Experimental data were supplemented by theoretical simulations.

LIMITS OF CONVECTIVE BURNING

When the pressure at the flame front exceeds the critical runaway pressure P_{CB}, convective burning arises. Low-velocity detonation arises when the pressure in the combustion wave exceeds the threshold value P_{LVD}, providing generation of hot spots due to visco-plastic deformation of pores. Convective burning is possible whenever the pressure in the combustion wave, P_x lies within the range $P_{CB} < P_x < P_{LVD}$.

METHODOLOGY OF THE STUDY OF STABILIZED CONVECTIVE BURNING

The essence of the approach systematically employed in our DDT studies is the separate exploration of the intermediate stages, CB and LVD. Through this, the limits of their existence are determined and the conditions governing stabilization of these propagation modes at controlled levels of propagation velocities and pressures are found. The use of the stabilized modes provided the benefit of

investigating long charges and significantly simplified obtaining and interpreting the experimental data.

The initial charge properties, including the EM type and reactivity, grain size, porosity, gas permeability, and the presence of various inhibiting additives, were varied within a wide range. The measurements provided a great body of data on the behavior of the process and enabled us to single out the key parameters controlling both its development and the characteristics to be compared with theoretical models. Of most importance is the fact that, in addition to individual parameters of the process, their dependencies on the initial properties were compared with those provided by theoretical models.

The following EM were studied:

- composite propellant (from now on propellant A) containing 78% ammonium perchlorate and 22% polyvinyl butyral binder with grains of various shape and size of effective diameter d_{ef} = 1.9, 0.96 and 0.66 mm,
- double-base propellant NB containing 40% nitroglycerine with d_{ef} = 0.81 mm,
- fine-grained single-channel pyroxylin propellant C with d_{ef} = 0.5 mm,
- PETN with d_{ef} = 0.5 mm.

The propellants studied had strong grains which were not destroyed under pressing the charges.

The following inert materials were used as inhibiting additives: paraffin (P), polyvinylbutyral (PVB), and ethylcellulose (EC). The additives were applied on the surface of an EM particle in the form of thin coatings by depositing them from solutions with subsequent drying. Charges with a preset porosity ranging between 2 and 15% were prepared by pressing (normally with no preheating).

EXPERIMENTAL FACILITIES AND TECHNIQUES, MEASURED PARAMETERS

To study the characteristics of stabilized CB, we used the set-up shown schematically in Fig. 1. The device comprises two sections: a cylindrical transparent high-pressure chamber with a tested charge and the afterburn section. The combustion chamber consists of a PMMA tube 15 or 18 mm in diameter. The tube is inserted tightly into a polished channel of a steel casing, in which a narrow slit is cut along the axis in order to photograph the process. Several orifices are drilled in the chamber along its axis in which high-frequency Kistler-type piezoquartz gauges are mounted. The afterburning section, 750 cm^3 in volume, is equipped

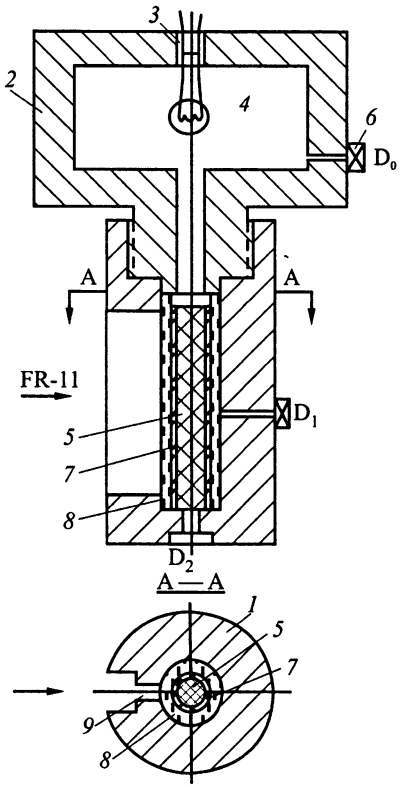

Figure 1 Schematic of the set-up designed to study stabilized convective burning: *1* — casing, *2* — afterburn section, *3* — nozzle, *4* — igniter, *5* — tested EM, *6* — piezoelectric pressure gauges (D_0, D_1, D_2), *7* — glycerine, *8* — PMMA tube, *9* — longitudinal slot

with the replaceable nozzle, which controls the outflow of the combustion products, and a piezoelectric pressure gauge. The process was initiated with an electric igniter cap, igniting a fast burning combustible mixture for producing a desired initial pressure in the chamber.

The set-up permitted the measurements to be conducted within a pressure range of up to 300 MPa. At the highest pressure, the inner PMMA tube was destroyed, but the steel casing with pressure gauges remained intact and was used repeatedly. The EM studied was pressed to produce pellets of a diameter which is slightly less than the inner diameter of the channel in the casing. The pellets were stacked to form a cylindrical charge of a length ranging from 70 to 200 mm. The side walls of the charge were coated with epoxy resin. After curing the resin, the charge was inserted into the channel of the casing and a small gap between the charge and casing walls was filled with glycerin. Electric signals from the pressure gauges were recorded on Data Lab digital recorder. Luminosity of the process was photographed with FR-11 and ZhFR-2 streak cameras differing in their sweep velocity.

Figure 2 shows the streak camera photographs of the pulsating quasisteady CB of propellant A. The corresponding pressure records and the procedure of joint processing of the piezometric and photographic data are exemplified in Fig. 3. From the measurements, the average flame velocity (W) (based on the slope of the luminous front track), average pressure in the afterburning section during flame propagation (P_b^*), pressure profiles at several sites along the charge length, the pressure at the flame front (P_f) (by matching the streak camera photographs and pressure signals), maximum pressure in the wave (P_x), the filtration zone thickness L_{fil} (based on the pressure profiles and velocity W), period T and amplitude (A_p) of the pressure pulses in the combustion chamber, and the mean step (h) of the jump-wise flame front displacement in camera

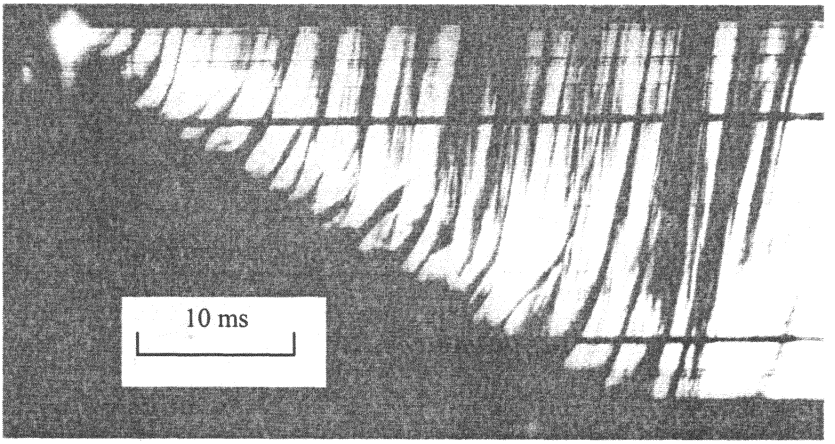

Figure 2 Streak photograph of pulsating quasisteady CB of propellant A+5% paraffin

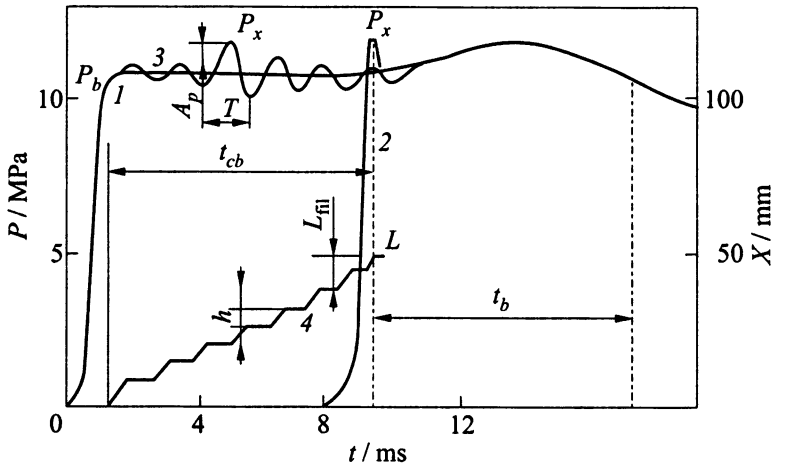

Figure 3 Schematic diagram illustrating the joint processing of streak photographs and pressure records for quasisteady convective burning: *1–3* — pressure–time histories recorded by gauges D_0, D_2, and D_1, respectively, *4* — trajectory of the flame front, A_p is the amplitude of pressure oscillations, T is the period of oscillations, h is the depth of flame front oscillations, t_{cb} is the time of convective burning propagation through the charge, t_b is the burning time of EM particles, and L_{fil} is the width of the filtration zone

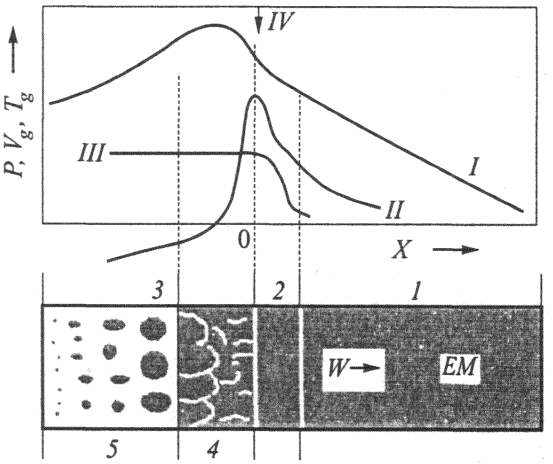

Figure 4 Schematic of the convective combustion wave structure in a low-porosity EM charge burning in a combustion chamber from which the combustion products are discharged: *1* — filtration zone, *2* — preheat zone, *3* — ignition and combustion zone, *4* — frontal part of the combustion zone, *5* — burn-down zone, *I* — pressure profiles, *II* — gas velocity, *III* — gas temperature, *IV* — flame front

photographs, were extracted. In addition, the pressure records in the afterburning section were used for estimating the burning time of EM particles (t_b), the burn-down zone length (L_b) and gas formation intensity in the CB-wave. The burning time (t_b) was measured as the difference between the start of the exponential pressure decay in the afterburning section and the instant when the flame spreads throughout the charge length, as determined from the joint processing of the pressure records and streak photographs. The gas formation intensity and the mean specific burning surface A_b were estimated from curve $P_b(t)$.

MECHANISMS AND CONDITIONS OF EXISTENCE OF QUASISTEADY CONVECTIVE BURNING IN LOW-POROSITY ENERGETIC MATERIALS

The spatial structure of a CB-wave and information on the profiles of the basic variables in burning low-porosity energetic materials, deduced from experimental and theoretical studies, are presented schematically in Fig. 4. The following spatial zones are distinguished: the filtration zone, where the cooled combustion products transfer their heat to the pore walls into which they have permeated and decelerated; the preheat zone, where the pore surface is heated to the ignition temperature due to convective heat transfer from the combustion products; and

Table 1 Basic characteristics of quasisteady convective burning of propellant A

EM	d_{ef} mm	P_b' MPa	W m/s	A_p MPa	T ms	L_{fil} mm	h mm	L_b mm	t_b ms
Propellant A	0.66	4.8	1.2	1.2	—	17	—	—	31
		10	4.7	2.0	2	6	9	—	23
	0.96	6	4.1	4	3.1	—	13	700	38
		11	9.3	5.2	1.4	24	12	800	30
	1.9	4.9	5.2	1.8	—	18	—	900	—
		9.2	11.3	2.0	1.9	16	22	1400	75
Propellant A + 5% P	0.96	14.6	23.5	2.8	—	21	—	1900	60
		11	1.4	1	11	30	16	—	52
		17	2.2	2.2	4.4	24	10	—	48
		17.6	2.2	2.2	4	—	8	—	—

Note: P is paraffin.

the ignition and combustion zone, where chemical conversion of EM begins in the ignition mode with subsequent regression (burning) of the pore surface. The interface between this latter zone and the preheat zone will be referred to as the ignition front, or the flame front. Here, the velocity of the gas flowing into the pores attains its maximum. Behind the flame front, the gas velocity decreases, and at the point, where the pressure peaks, passes through zero and changes its sign. This point can be referred to as the flow separation point.

An idea about the burn-down zone length can be found from estimates of parameter L_b listed in Table 1. Although the EM in this zone undergoes chemical transformation in the regime of layer-by-layer burning over the surface of ignited pores, the flame rapidly covers a vast area due to the difference between the rates of layer-by-layer and convective burning, which may be as large as 1000-fold. It is the extended burn-down zone with a well developed surface area, which is responsible for the high propensity of CB to acceleration due to the feedback through the pressure build-up.

The major result of this study is the proof of the fact that by affecting the burning zone one can slow down the evolution of an explosion process and, under certain conditions, even stabilize it at the CB stage. The burning process is affected via two ways: (i) dynamic unloading of the burning zone due to outflow of the reaction products to an afterburning chamber equipped with a nozzle, and (ii) decrease in the intensity of chemical conversion by diminishing the burning surface area due to a decrease in the specific surface area of EM particles and due to coating the particle surface with films of inert materials.

The data on the filtration zone thickness L_{fil} are listed in Table 1. The representative L_{fil} values range between 15 and 30 mm. The attempts to find a correlation between L_{fil} and any other parameters were failed. On the contrary,

the fluctuating characteristics of the burning process are closely related, as seen from the data presented in the same table, to the pressure and CB velocity. Generally speaking, the higher the pressure and the CB velocity, the greater are the amplitude (A_p) and frequency ($1/T$) of the pressure fluctuations and shorter is the length of flame hops (h).

The conditions needed for stabilizing CB in the experimental device with an afterburning section can be formulated as follows:

1. The initial porosity and gas permeability of a charge should not exceed the threshold values equal to about 15% and 10^{-7} cm^2, respectively. When the porosity and gas permeability of charges were higher, we failed to stabilize the pressure in the afterburning section and the burning velocity by varying the nozzle throat. The process proceeded with an appreciable increase in the flame velocity with time, throughout the major portion of the charge, and a decrease in the velocity, as the flame approached the closed rear charge end.

2. The pressure range, within which CB was stabilized, is bounded by the upper and lower boundaries. These boundaries can be compared with the threshold pressures P_{CB} and P_{LVD}.

An analysis of the mechanism of quasisteady CB has shown that the important factor, which allows the process to be stabilized by constraining the pressure rise in the burning zone, is the periodic dispersion of burning EM under tensile stresses arising from the outflow of the combustion products. Because of dispersion, the flame speed and pressure fluctuate, but their average values remain nearly constant.

CONTROL OF PROPAGATION OF QUASISTEADY CONVECTIVE BURNING IN LOW-POROSITY ENERGETIC MATERIALS

Further studies were aimed at understanding the effect exerted on the basic characteristics of quasisteady combustion waves by such parameters as the pressure in the afterburning section P_b' (the mean pressure at the "shelf" portion), initial particle size, charge porosity, and inhibitor content. The results of measurements for propellant A, at a 5% charge porosity, are summarized in Table 1.

Consider the pressure dependence of the quasisteady convective burning velocity. Figure 5 shows the CB velocity as a function of the maximum pressure for three different EM: PETN, double-base propellant NB, and composite propellant A. Propellant A has the highest burning velocities, whereas PETN exhibits the strongest pressure dependence of the burning velocity. From the above data,

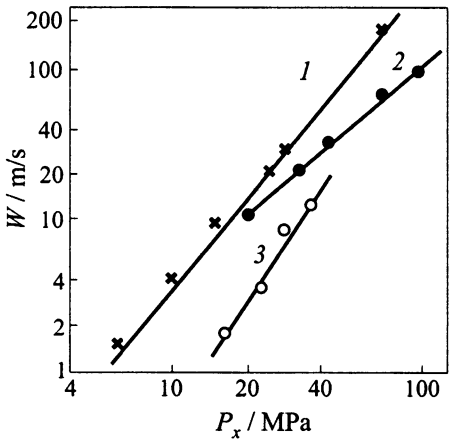

Figure 5 Pressure dependence of the quasisteady burning velocity for three EM: *1* — propellant A (d_{ef} = 0.96 mm; *2* — double base propellant NB (d_{ef} = 0.9 mm); *3* — PETN (d_{ef} = 0.5 mm)

treated in the form of a power dependence $W = B_c P_x^{\nu_c}$, we infer that in the row: PETN, propellant A, and propellant NB — ν_c equals to 2.7, 2.0, and 1.45, respectively. There is no correlation between the convective and layer-by-layer burning modes in the velocity values and pressure exponent.

Table 2 lists more comprehensive data on coefficients B_c and ν_c, which control the pressure dependence of the CB velocity. The table also presents the burning velocities at a pressure of 20 MPa and in the pressure range relevant to current measurements.

The effect of the initial porosity on the pressure dependence of the CB velocity is illustrated in Fig. 6 for propellant A. As is seen, an increase in φ_0 raises W and does not affect ν_c. With rising d_{ef}, W increases, whereas ν_c decreases.

Figure 7 shows the velocity of CB as a function of pore diameter for propellant A at two pressure levels. By and large, although the data are scattered, a trend to larger velocities with increasing the pore diameter is clearly seen.

Table 2 Velocity of quasisteady convective burning and its pressure dependence

EM	d_{ef} mm	B_c	ν_c	W, m/s, at P_c' = 20 MPa	Pressure range MPa
PETN	0.5	8.8×10^{-4}	2.7	2.9	10–15
Propellant A	1.9	0.23	1.6	20.6	4–60
	0.96	0.040	2.0	16	5–70
	0.66	0.0214	2.2	15.6	6–90
A + 3% P	0.96	0.132	1.1	3.6	8–20
A + 5% P	0.85	0.19	0.8	2.1	4–20
A + 5% EC	0.85	1.0	0.45	3.9	5–50
Propellant NB	0.82	0.15	1.45	11.5	20–90
NB + 3% PVB	0.82	0.95	0.8	10.4	20–100
Propellant C + 7.5% PVB	0.5	1.05	0.53	5.1	30–160

Note: PETN charges have porosity of 10%, other charges have porosity of 5%; P is paraffin, EC is ethyl cellulose, and PVB is polyvinyl butyral.

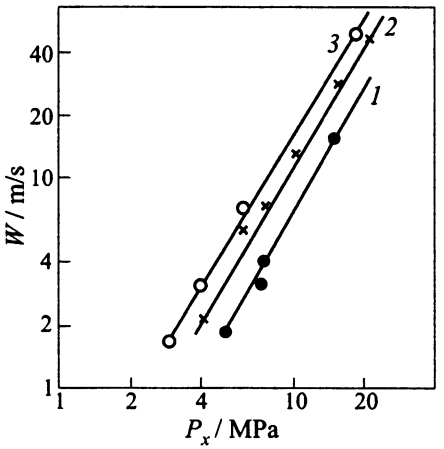

Figure 6 The effect of the initial porosity φ_0 on the pressure dependence of the convective burning velocity for propellant A (d_{ef} = 1.9 mm): *1* — φ_0 = 2%, *2* — 5%, *3* — 12%

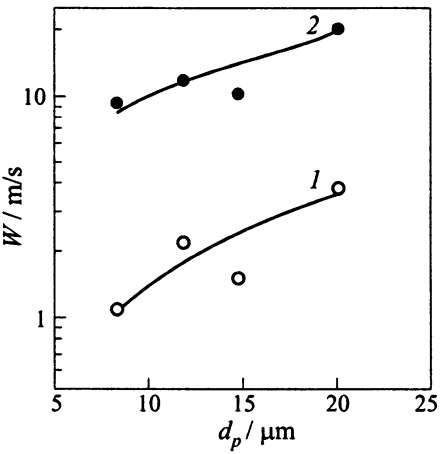

Figure 7 The correlation between the convective burning velocity and pore diameter for propellant A at *1* — P_x = 6 MPa and *2* — 16 MPa

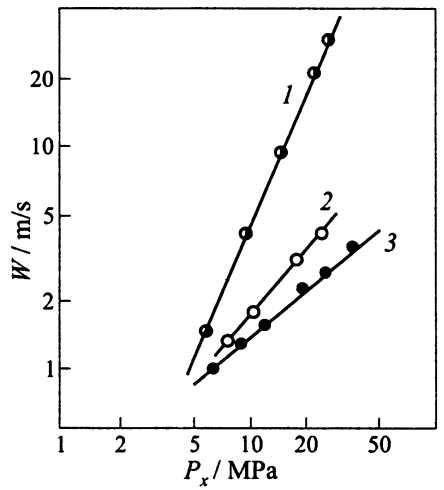

Figure 8 The effect of paraffin additives on the velocity of convective burning of propellant A (d_{ef} = 0.96 mm) at a 5% porosity: *1* — A, *2* — A + 3% paraffin, *3* — A + 5% paraffin

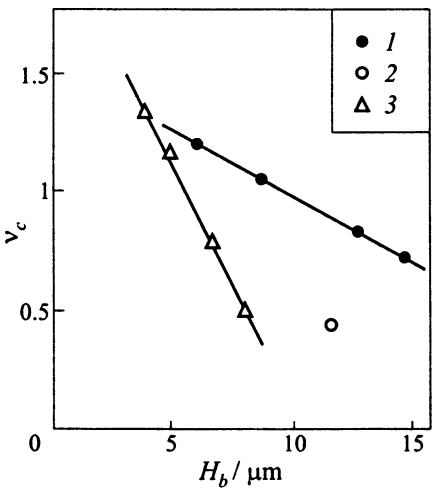

Figure 9 Correlation between the adiabatic exponent ν_c and the binder film thickness: *1* — paraffin, *2* — ethyl cellulose, *3* — polyvinyl butyral

The effect of inhibitor additives was also analyzed. As is seen from Fig. 8, introduction of paraffin significantly reduces the CB velocity and exponent ν_c, with the latter quantity dropping below unity. The inhibitor effect increases with the amount of additive introduced. Similar data were obtained for the other EM, which exhibits no break of granules during charge preparation.

Comparison of various inhibitors has demonstrated that the inhibiting effect tends to rise for additives with higher thermal stability.

The analysis of the above data indicates that the thicker the inhibitor film on the particle surface, the more pronounced is the inhibiting effect. The graph demonstrating this result is shown in Fig. 9. Thus, to obtain the same inhibiting effect with smaller particles, one should increase the additive content.

THEORETICAL MODELING OF QUASISTEADY CONVECTIVE BURNING

A Model of Pulsating Quasisteady Convective Burning

The model is based on the above-discussed experimental observations of periodic pressure fluctuations, jump-wise flame front propagation, and dispersion of EM charges in the course of their quasisteady CB. The basic factors that contribute to CB stabilization in low-porosity EM are the periodical dispersion of the burning charge fraction and removal of burning fragments, both limiting the pressure rise. The calculation results from this model [5, 9] are compared with the available experimental data.

The dependencies predicted by this model for the characteristics of pulsating burning mode are compared with experimental findings in Table 3. The agreement can be considered to be satisfactory. Thus, the results of modeling support the hypothesized pulsating mechanism of quasisteady CB.

APPLICATIONS OF THE HIGH-SPEED CONTROLLED CONVECTIVE BURNING OF THE COMPACTED LOW-POROSITY PROPELLANTS

Convective burning of low-porosity charges makes it possible to achieve well-controlled high rates of chemical energy release in the charge and to increase 1.5- or 2-fold the energy concentration per unit volume of the chamber, as compared to the traditional burning modes in pulsed rocket motors and guns. Our investigations laid scientific and practical grounds for solving this problem.

Table 3 Experimental and theoretical relations for quasisteady pulsating CB

Characteristics of pulsating quasisteady burning	Experiment	Theoretical modeling
Convective burning velocity W	$W \propto P_x^{\nu_c}$, $\nu_c = 1.6$–2.8 $W \uparrow$, if $d_p \uparrow$ and $\sigma_R \uparrow$	$W_0 \propto d_p A_p^{3/2} P_f^{(\nu_c+1/2)}$
Period of fluctuations T	$T \propto P_x^{-1\,5}$ and $\neq f(d_p)$ $T \downarrow$ if $\sigma_R \uparrow$	$T \propto A_p^{-1} P_f^{-2\nu_c}$ and $\neq f(d_p)$
Amplitude of fluctuations A_p	$A_p \uparrow$ if $\sigma_R \uparrow$ and $P_x \uparrow$	$A_p \uparrow$ if $\sigma_R \uparrow$ and $\neq f(P_f)$
Pitch at the acceleration stage h	$h \propto d_{ef}$, $h \downarrow$ if $P_x \uparrow$	$h \propto d_p A_p^{1.2} P_f^{(1/2-\nu_c)}$

Note: P_x is the maximum pressure in the convective burning wave, P_f is the pressure at the flame front.

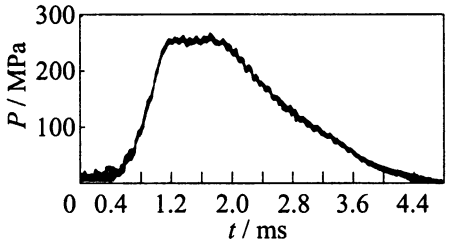

Figure 10 The pressure–time diagram with a plateau in 23 mm barrel system

To study ignition, convective burning, and internal ballistics of low-porosity energetic materials, the experimental measuring facilities were designed and manufactured to perform complex studies under conditions simulating intrachamber processes at pressure of up to 400 MPa. The studies performed have demonstrated fundamental feasibility of a significant increase (up to 1.4 g/cm^3) of the loading density in pulse rocket motors and guns, and of obtaining reproducible pressure–time histories of a controlled flat-top shape (Fig. 10). The use of compacted high-progressive low-porosity charges in cartridges increases the projectile velocity up to 20% (as compared to the traditional charges), when maximum pressure of shot is invariable.

CONCLUDING REMARKS

In this paper,

- comprehensive data on the stabilization conditions and characteristics of stabilized convective burning are obtained,
- stabilization mechanisms are studied,

Table 4 Effect of control factors on the basic characteristics of quasisteady CB

Parameters	Initial porosity	Particle size	Inhibitor additives	Thermal stability of additive	Layer-by-layer burning velocity	Charge strength
P_{CB}	↓↓	↓	↑	?	↓↓	~
P_{LVD}	~	?	↑	?	?	
W	↑	↑↓	↓↓	↓	~	?
ν_c	~	↓	↓↓	↓	~	?
t_b	↓	↑	↑↑	↑	↓↓	↑
A_b	↑↑	↓	↓↓	↓		↑

Note: ↑ signifies that an increase in the factor indicated in the column entails an increase in the parameter indicated in the row, ↓ means the reverse effect. Double arrow indicates that the effect is strong; ~ points to the lack of influence; ? indicates that the dependence is not firmly established.

- factors controlling the CB stability and characteristics are ascertained, and
- theoretical models for explaining experimental observations and checking the underlying hypotheses are developed.

Table 4 summarizes the effects of various factors on the limits and basic characteristics of quasisteady CB. The strongest remedy is the use of inhibiting films coating EM grains. The effect of inhibitors manifests itself both at the stage of flame propagation and during burning of dispersed EM particles. Inhibiting additives efficiently reduce the convective burning velocity, its pressure dependence, and intensity of the reaction within the burning zone. Of particular interest is a possibility of reducing the pressure exponent ν_c to values below unity. The mechanism of the effect exerted by the inhibitors consists in ignition delaying by the inert coating. The effect is enhanced as the film thickness and thermal resistance increase.

Among other factors, one can single out the initial charge porosity (its variation allows controlling such parameters as the low limit of quasisteady convective burning, burning intensity, and flame speed) and the size of EM particles (its variation affects all the characteristics of convective burning, except, may be, for the upper limit of convective burning).

ACKNOWLEDGMENTS

This work was supported by the Russian Foundation for Basic Research, project No.97-03-32051.

REFERENCES

1. Belyaev, A. F., Bobolev, V. K., Korotkov, A. I., Sulimov, A. A., and Chuiko, S. V., *Deflagration-to-Explosion Transition in Condensed Systems.* Nauka, Moscow, 1973.
2. Taylor, T. W., *Combustion Flame*, **6**, 103, 1962.
3. Andreev, K. K., and Chuiko, S. V., *Sov. J. Physical Chemistry*, **37**, 6, 1034, 1963.
4. Cole, R. A., and Fifer, J. E., *Proc. 7th Symposium (International) on Detonation*, CPIA Publications, Annapolis, MD, **1**, 1981, 164.
5. Ermolaev, B. S., Sulimov, A. A., Foteenkov, V. A., *et al.*, *Sov. J. Physics Combustion Explosion*, **16**, 3, 24, 1980.
6. Khrapovskii, V. E., and Sulimov, A. A., *Sov. J. Physics Combustion Explosion*, **24**, 2, 39, 1988.
7. Roman'kov, A. V., Sulimov, A. A., Sukoyan, M. K., and Biryukov, M. S., *Sov. J. Chemical Physics*, **11**, 7, 983, 1992.
8. Sulimov, A. A., Ermolaev, B. S., Borisov, A. A., *et al.*, *Proc. 6th Symposium (International) on Detonation*, Arlington, VA, 1976, 250.
9. Sulimov, A. A., and Ermolaev, B. S., *Rus. J. Chemical Physics*, **16**, 10, 1997.